14 Mar 1991, 10:30 am - 12:30 pm

Dynamic Strength and Permanent Deformation of Saturated Sand

Masayuki Hyodo
Yamaguchi University, Japan

Noriyuki Yasufuku
Yamaguchi University, Japan

Hidekazu Murata
Yamaguchi University, Japan

Takeharu Konami
Yamaguchi University, Japan

Proceedings: Second International Conference on Recent Advances in Geotechnical Earthquake Engineering and Soil Dynamics, March 11-15, 1991, St. Louis, Missouri, Paper No. 3.36

Dynamic Strength and Permanent Deformation of Saturated Sand

Masayuki Hyodo
Associate Professor of Civil Engineering, Yamaguchi University, Ube, 755, Japan

Noriyuki Yasufuku
Research Associate of Civil Engineering, Yamaguchi University, Ube, 755, Japan

Hidekazu Murata
Professor of Civil Engineering, Yamaguchi University, Ube, 755, Japan

Takeharu Konami
Graduate Student of Civil Engineering, Yamaguchi University, Ube, 755, Japan

SYNOPSIS: The undrained cyclic triaxial behaviour of saturated sand has been studied using anisotropically consolidated specimens. The strength and deformation under various combination of initial static and cyclic shear stresses were attempted to clarify. The cyclic strength was first discussed, and then, the residual shear strain was investigated related with effective stress ratio at the end of each stress cycle. Finally, an empirical model was proposed for evaluating the development of pore pressure and residual shear strain of saturated sand subjected to various initial static and subsequent cyclic shear stresses.

INTRODUCTION

It is recognized that the behaviour of soil elements in slopes or ground underneath structures composed of saturated sands is different from that of level ground during cyclic loading because the soil elements are generally subjected to an initial static shear stress on a horizontal plane or assumed failure surface (Lee and Seed, 1967, Yoshimi and Oh-oka, 1975, Vaid and Chern, 1983). The behaviour of saturated sand in such stress condition is not clear because it varies in a complicated manner related to the magnitude of initial static and subsequent cyclic shear stresses. The purpose of this study is to define the unified cyclic strength of saturated sand with various magnitudes of initial static shear stress. A further aim of this study is to quantify the pore pressure and the residual shear strain and to develop a model for evaluating them. Cyclic triaxial tests were carried out in a series of different initial static and cyclic shear stresses.

TEST PROGRAM

Toyoura sand, a subangular, fine sand was used in this study. Its index properties are G_s=2.64, D_{50}=0.18mm, U_c=1.20, e_{max}=0.973, e_{min}=0.635. A sinusoidal cyclic axial load was applied at a frequency of 0.1Hz under undrained conditions. Cyclic loading tests were performed on both isotropically and anisotropically consolidated samples with a relative densities of 50%. The tests for another relative density (Dr=70%) were also done but they were shown in the other paper (Hyodo et al, 1989). Cyclic loading tests were performed over a range of initial static deviator stresses q_s varying from 0 to 80kPa at 10 kPa intervals. About four to six magnitudes of cyclic deviator stress q_{cyc} were combined with each static deviator stress so that both reversal and no reversal of cyclic shear stresses were simulated.

TEST RESULTS

3.1 Cyclic Behaviour of Anisotropically Consolidated Sand

Typical effective stress paths during cyclic loading for sand in each loading patern are shown in Fig.1. The failure envelope obtained from monotonic loading tests is also drawn in this figure. In the case of reversal the ef-

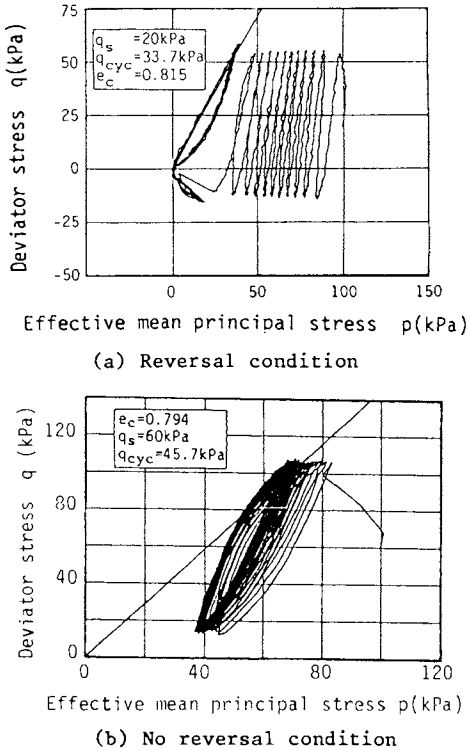

Fig.1 Typical effective stress path for reversal and no reversal conditions

fective stress path moved towards the failure envelope during cyclic loading and finally it traced a steady loop beside the failure envelope. On the other hand, in the no reversal case, the effective stress path moved until the upper end of it touched the failure line.

Typical results demonstrating the relationship between cyclic deviator stress and axial strain are presented in Fig.2. While a large amplitude of cyclic axial strain was observed in the case of stress reversal, in the no reversal case, residual strain was predominant instead of cyclic strain.

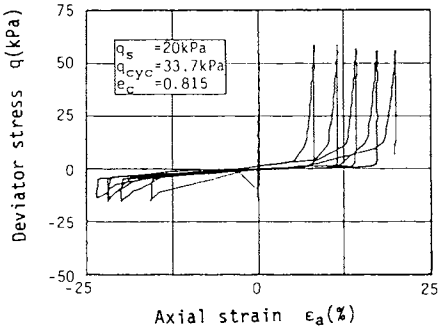

(a) Reversal condition

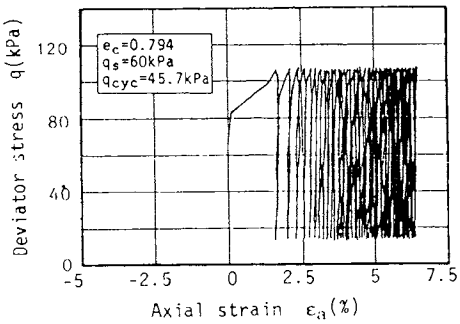

(b) No reversal condition

Fig.2 Typical deviator stress and axial strain relationship

3.2 A Unified Definition of Cyclic Shear Strength

It is convenient to make a unified definition of cyclic shear strength in both reversed and unreversed stress conditions. In the condition of reversal, development of DA=5%(double amplitude of cyclic axial strain =5%) was looked upon as a failure as a proof of liquefaction. On the other hand, in the unreversed condition, cumulative residual strain progressed, and so the occurrence of RS=10%(magnitude of residual strain =10%) was regarded as a failure, by considering of usual static failure criteria. Taking 10% of residual axial strain (RS=10%) as a failure criterion in both reversal and no reversal regions, cyclic strength can be approximated as curves in Fig.3, in which for comparison, the strength curves based on DA=5% are also drawn by broken lines. Although the criterion based on RS=10% may be felt to slightly overestimate the cyclic strength in the reversal side, it is possible to approximate the cyclic strength for practical use. Then RS=10% was adopted as a unified cyclic failure criterion in both reversal and no reversal stress regions. The cyclic strength curves based on this criterion can be approximated by straight lines in logarithmic form as shown in Fig. 4. These are given by parallel straight lines for each initial static shear stress and then formulated as follows.

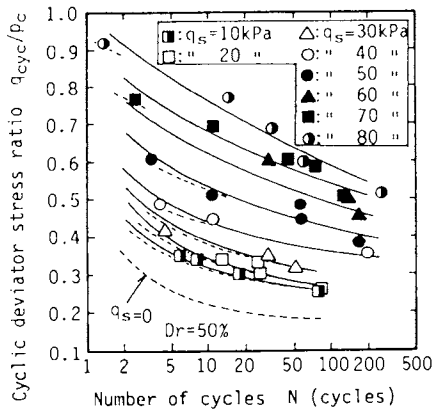

Fig.3 Relatioship between cyclic deviator stress ratio and number of cycles to induce RS=10%

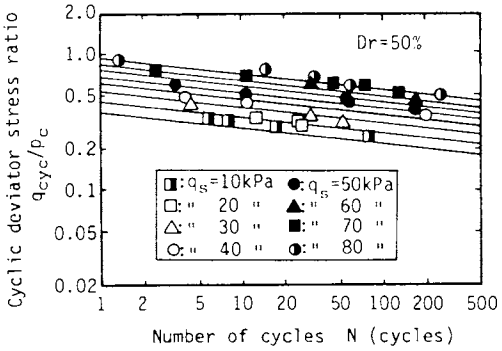

Fig.4 Cyclic strength lines in logarithmic diagram

$$q_{cyc}/p_c = \kappa N^{\beta} \qquad (1)$$

$$\beta = -0.115, \quad \kappa = 0.297 + 0.804\, q_s/p_c$$

3.3 Evaluation of Residual Axial Strain

Attempts were made to quantify the residual pore pressure and axial strain which were measured at the end of each loading cycle. Residual strains from all tests were related using an effective stress ratio, $_r(=q_s/p)$ which is the value of initial static shear stress divided by mean effective principal stress of each end of stress cycle. Fig.5 shows the relationship between residual axial strain and effective stress ratio. It is found that in spite of varying initial static and cyclic shear stresses, there is a unique relationship between them which can be approximated by a hyperbola. It is observed in the figure that the residual strain grows rapidly just before failure although it keeps fairly small quantity before the effective stress path approaches the failure envelope.

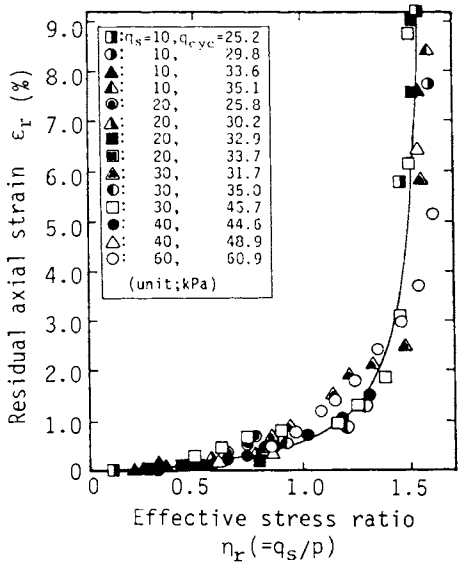

(a) Reversal

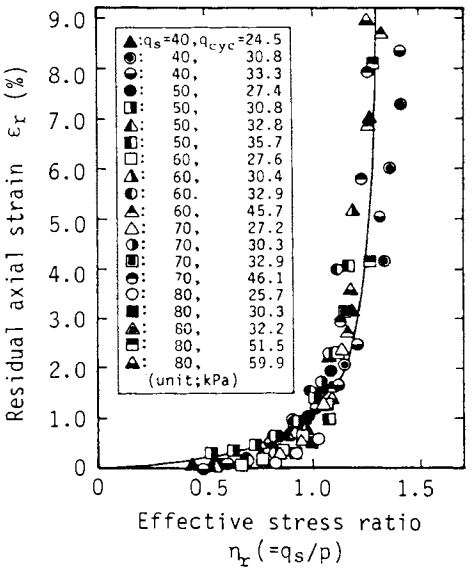

(b) No reversal

Fig.5 Relationship between residual axial strain and effective stress ratio at the end of each stress cycle

In the reversal condition, the result is presented in Fig.5(a). In the case of no reversal, as shown in Fig.5(b), the strain grows rapidly from a little smaller effective stress ratio comparing with the former. The relations shown in Fig.5 were formulated as the following equation.

$$\varepsilon_r = \eta_r/(b-c\eta_r) \qquad (2)$$

where b and c are coefficients determined from experimental data. The values of the coefficients b and c determined by regression analysis of the test data are summarized in Table 1.

Table 1 Summary of coefficients b and c

	Coefficient b	Coefficient c
Reversal	11.590	7.624
No reversal	3.860	2.860

3.4 New Cyclic Effective Stress Ratio versus Cyclic Shear Strength Ratio

In the previous section, a unified cyclic shear strength q_{cyc}/p_c, applicable to the all loading patterns was defined. A new expression R/R_f was introduced, which is the ratio of an amplitude of cyclic shear stress and cyclic shear strength in a given number of loadings. R/R_f, named cyclic shear strength ratio, is equivalent to a reciprocal of the safety factor against cyclic failure. When a cyclic load with uniform amplitude R in a given initial static shear stress is applied, the cyclic strength R_f corresponding to the initial static shear stress and the number of cycles is selected and R/R_f is evaluated. The value of R/R_f increases with the increase of number of cycles until it equals unity because R is constant and R_f decreases with number of cycles.

Next, a new cyclic effective stress ratio, η^* was defined as the following equation.

$$\eta^* = \frac{\eta_r - \eta_s}{\eta_f - \eta_s} \qquad (3)$$

where η_r is an effective stress ratio at the end of a given number of cycles, η_s is the effective stress ratio of initially anisotropically consolidated condition and η_f is the effective stress ratio at the failure. Therefore, η^* means the situation at the end of a given cycle relative to initial and failure states in p-q diagram. Fig.6 shows the relationship between η^* and R/R_f at number of cycles N=10, 20 and 30 together. It is recognized in the figure that there exists a unique relationship between η^* and R/R_f in the same initial static shear stress condition. It is also found that although the relation depends on initial static shear stress, it is independent of magnitude and number of cyclic loadings. They can be formulated as the following equation.

$$\eta^* = \frac{(R/R_f)}{\{\, a - (a-1)R/R_f \,\}} \qquad (4)$$

in which a is an experimental parameter and is related by the initial static shear stress ratio as shown in Fig.7. The finding of this relationship have made possible to develop a procedure for evaluating the pore pressure and residual strain in cyclic loading.

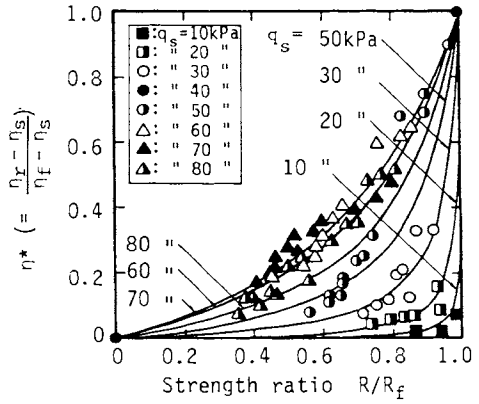

Fig.6 Relationship between effective stress ratio η^* and strength ratio R/R_f

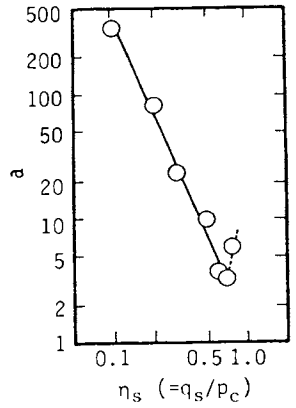

Fig.7 Relationship between parameter a and initial static shear stress ratio η_s

PREDICTION OF RESIDUAL PORE PRESSURE AND RESIDUAL AXIAL STRAIN

Residual pore pressure and residual axial strain in each stress cycle was predicted by using the following process.

(1) Cyclic shear strength, R_f, for the desired initial static shear stress and number of stress cycles was decided through the relationship given by Eq.(1). Then the value of cyclic shear strength ratio R/Rf, was obtained by dividing applied cyclic shear stress R by the strength R_f.

(2) The effective stress ratio η^* was obtained by substituting R/R_f into the relation between η^* and R/R_f given by Eq.(4).

(3) The effective stress ration η_r at the end of a given stress cycle was calculated by the following variation form of Eq.(3).

$$\eta_r = \eta^*(\eta_f - \eta_s) + \eta_s \qquad (5)$$

(4) The residual pore pressure was calculated from the value of η_r by using the following equation.

$$u_r = p_c - q_s/\eta_r \qquad (6)$$

(5) The residual axial strain was evaluated by substituting η_r into the relation given by Eq.(2).

These steps were continued from the first to the end of stress cycle. The predicted and experimental residual pore pressure is presented in Fig.8. In this figure, predicted and experimental results correspond to plots and solid lines, respectively. It is recognized there are reasonably good correspondences between predicted and experimental results especially in their initial quantities, sudden increases at the certain number of cycles near the occurrence of liquefaction in the reversal stress condition and their final convergences to the constant values.

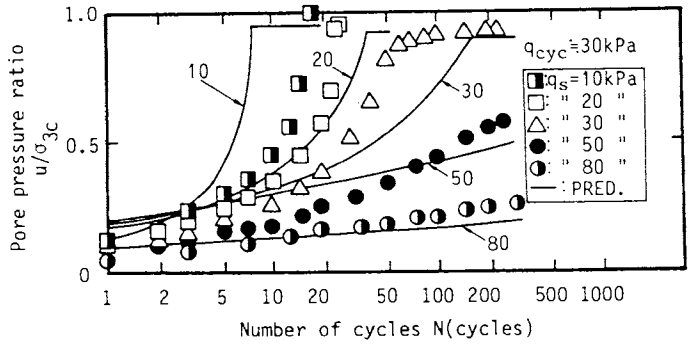

(a) Case of q_{cyc}=30kPa with various q_s

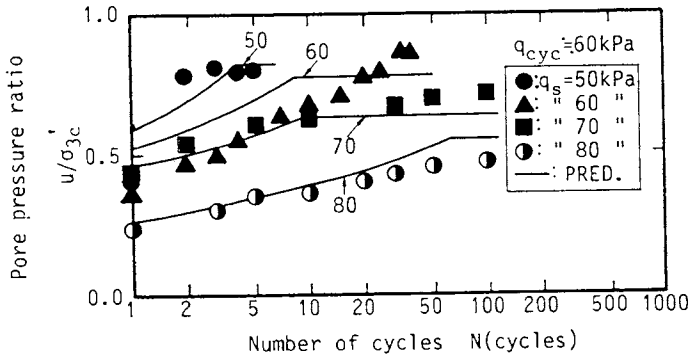

(b) Case of q_{cyc}=60kPa with various q_s

Fig.8 Predicted and experimental residual pore pressure ratio

The same comparison are also done for residual axial strains. Fig.9 shows predicted and experimental residual axial strains. It is also found there are good correspondences between them especially in their sudden development near the failure in reversal condition and their gradual increase in no reversal state.

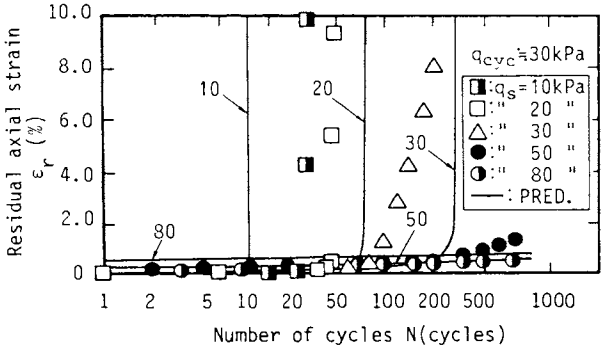

(a) Case of q_{cyc}≒30kPa with various q_s

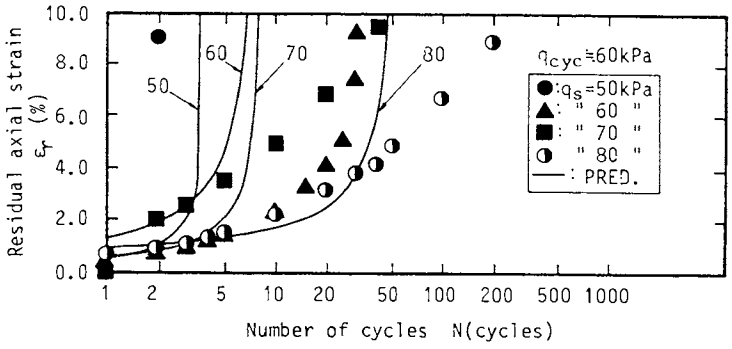

(b) Case of q_{cyc}≒ 30kPa with various q_s

Fig.9 Predicted and experimental residual axial strain

APPLICATION OF VARIABLE AMPLITUDE OF CYCLIC SHEAR STRESS

The proposed procedure for evaluating the pore pressure and residual strain was applied to the cyclic behaviour of soil subjected to variable amplitude of cyclic shear stresses. Cyclic triaxial test was carried out applying the variable amplitude of cyclic shear stress as shown in Fig.10. The applied cyclic shear stress of each stage is summarized in Table 2. It was of unreversed condition at the first and the second each five cycle, and then of reversal one at the third and the last stages. Fig.11 and Fig.12 show the effective stress path and deviator stress and axial strain relationship, respectively. There are very unique and interest features of the behaviour of sand from the initial state to the failure condition in these figures. It was also observed in these figures that the pore pressure and axial displacement growed up rapidly at the start of third stage when the reversal cyclic load was started. It is noted that the axial displacement growed to the compression side as the residual one in the third stage and that it changed to become a cyclic one at the last stage.

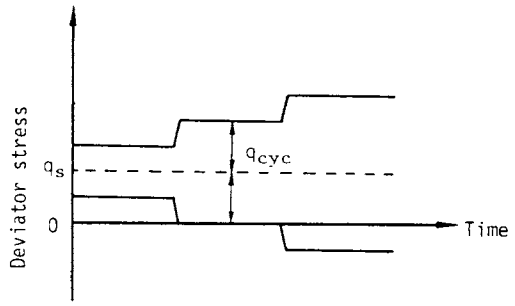

Fig.10 Variable amplitude of cyclic shear stress (schematic)

Table 2 Test condition for variable amplitude cyclic triaxial test

q_s(kPa)	q_{cyc}(kPa)			
	N=1~5(cycle)	N=6~10(cycle)	N=10~15(cycle)	N=15~20(cycle)
30	18.3	23.0	30.9	40.5

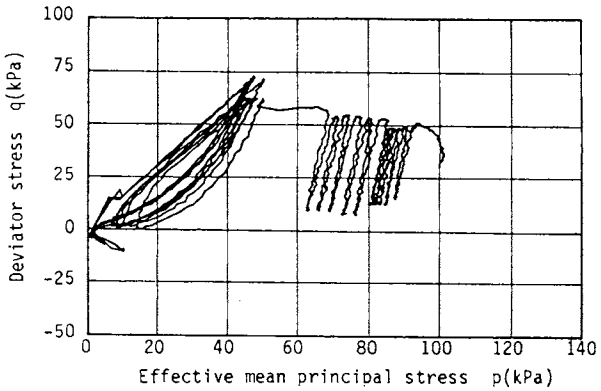

Fig.11 Effective stress path of sand tested

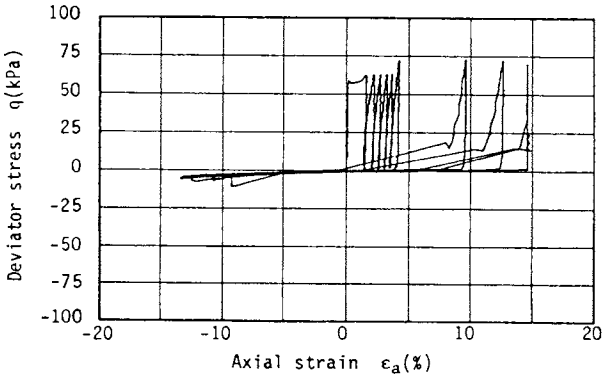

Fig.12 Deviator stress and axial strain relationship of sand tested

Then prediction of residual pore pressure and residual axial strain was performed by the following procedure.

(1) In the part of first amplitude of cyclic stress ratio R_1, the same procedure was used with the case of uniform cyclic stress.

(2) When we consider that after the N cycles of first part of cyclic stress, the cyclic stress ratio with the second amplitude R_2 follows, N is corrected to N' by the following equation.

$$N' = N(R_2/R_1)^{1/\beta} \qquad (7)$$

where ß is the slope of cyclic strength lines given by Eq.(1). N' is looked upon as the equivalent number of cycles for the second amplitude of cyclic stress. Then the second part is considered to start from (N'+1) cycle. Experimental and predicted pore pressure and residual axial strain were presented in Fig.13 and 14, respectively. It is noted that there are reasonable correspondences between them. Therefore, the proposed model is also applicable to the anisotropically consolidated soil behaviour subjected to variable amplitudes of cyclic shear stresses.

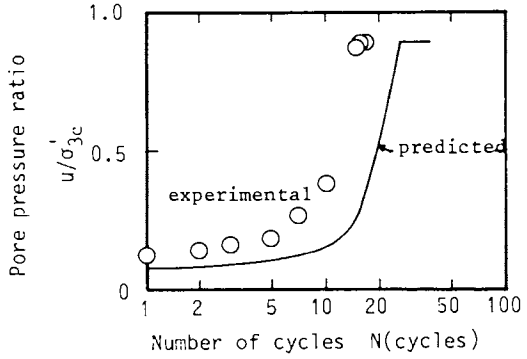

Fig.13 Predicte and experimental residual pore pressure ratio

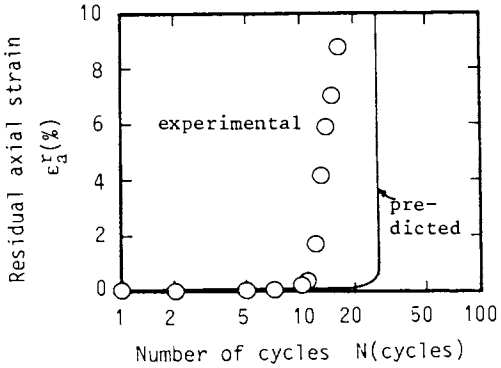

Fig.14 Predicted and experimental residual axial strain

CONCLUSIONS

In order to evaluate the characteristics of cyclic shear strength and deformation of saturated sand with initial static shear stress subjected to cyclic loading, the cyclic triaxial compression tests were performed with varying the initial static and subsequent cyclic shear stresses. Based on the experimental results, an empirical model for evaluating the development of pore pressure and residual axial strain was estabished.

REFFERENCES

Hyodo, M., H. Murata, N. Yasufuku, T. Fujii (1989), "Undrained cyclic shear strength and deformation of sands subjected to initial static shear stress", Proc. of 4th International Conference on Soil Dynamics and Earthquake Engineering, Mexico-city, pp.81-103.

Lee, K.L. and H.B. Seed (1967), "Dynamic strength of anisotropically consolidated sand", Proc.ASCE, Vol.93, No.SM5, pp.169-190.

Yoshimi, Y. and H. Oh-oka (1975), "Influence of degree of shear stress reversal on the liquefaction potential of saturated sand", Soils and Foundations, Vol.15, No.3, pp.27-40.

Vaid, Y.P. and J.C. Chern (1983), "Effect of static shear on resistance to liquefaction", Soils and Foundations, Vol.23, No.1, pp.47-60.